

## Correlation between the $^{12}\text{C}+^{12}\text{C}$ , $^{12}\text{C}+^{13}\text{C}$ , and $^{13}\text{C}+^{13}\text{C}$ fusion cross sections

M. Notani,<sup>1,\*</sup> H. Esbensen,<sup>2</sup> X. Fang,<sup>1</sup> B. Bucher,<sup>1</sup> P. Davies,<sup>3</sup> C. L. Jiang,<sup>2</sup> L. Lamm,<sup>1,†</sup> C. J. Lin,<sup>4</sup> C. Ma,<sup>1</sup> E. Martin,<sup>3</sup> K. E. Rehm,<sup>2</sup> W. P. Tan,<sup>1</sup> S. Thomas,<sup>3</sup> X. D. Tang,<sup>1,‡</sup> and E. Brown<sup>5</sup>

<sup>1</sup>*Department of Physics, Institute for Structure and Nuclear Astrophysics, and the Joint Institute for Nuclear Astrophysics, University of Notre Dame, Notre Dame, Indiana 46556, USA*

<sup>2</sup>*Physics Division, Argonne National Laboratory, Argonne, Illinois 60439, USA*

<sup>3</sup>*Department of Physics, University of Surrey, Guildford, Surrey GU2 7XH, United Kingdom*

<sup>4</sup>*China Institute of Atomic Energy, P.O. Box 275(10), Beijing 102413, People's Republic of China*

<sup>5</sup>*Department of Physics & Astronomy, National Superconducting Cyclotron Laboratory, and the Joint Institute for Nuclear Astrophysics, Michigan State University, East Lansing, Michigan 48824, USA*

(Received 9 July 2011; revised manuscript received 22 December 2011; published 17 January 2012)

The fusion cross section for  $^{12}\text{C}+^{13}\text{C}$  has been measured down to  $E_{\text{c.m.}} = 2.6$  MeV, at which the cross section is of the order of 20 nb. By comparing the cross sections for the three carbon isotope systems,  $^{12}\text{C}+^{12}\text{C}$ ,  $^{12}\text{C}+^{13}\text{C}$ , and  $^{13}\text{C}+^{13}\text{C}$ , it is found that the cross sections for  $^{12}\text{C}+^{13}\text{C}$  and  $^{13}\text{C}+^{13}\text{C}$  provide an upper limit for the fusion cross section of  $^{12}\text{C}+^{12}\text{C}$  over a wide energy range. After calibrating the effective nuclear potential for  $^{12}\text{C}+^{12}\text{C}$  using the  $^{12}\text{C}+^{13}\text{C}$  and  $^{13}\text{C}+^{13}\text{C}$  fusion cross sections, it is found that a coupled-channels calculation with the ingoing wave boundary condition (IWBC) is capable of predicting the major peak cross sections in  $^{12}\text{C}+^{12}\text{C}$ . A qualitative explanation for this upper limit is provided by the Nogami-Imanishi model and by level density differences among the compound nuclei. It is found that the strong resonance found at 2.14 MeV in  $^{12}\text{C}+^{12}\text{C}$  exceeds this upper limit by a factor of more than 20. The preliminary result from the most recent measurement shows a much smaller cross section at this energy, which agrees with our predicted upper limit.

DOI: [10.1103/PhysRevC.85.014607](https://doi.org/10.1103/PhysRevC.85.014607)

PACS number(s): 25.70.Jj, 24.30.-v, 25.70.Ef, 25.70.Gh

### I. INTRODUCTION

In 1960 Almqvist, Kuehner, and Bromley discovered several resonances in collisions between  $^{12}\text{C}$  nuclei. For at least three energies,  $E_{\text{c.m.}} = 5.68, 6.00,$  and  $6.32$  MeV, they observed increased yields for the reaction products  $p, \alpha, n,$  and  $\gamma$ . These resonances have characteristic widths of about 100 keV and were interpreted as signatures for the formation of nuclear molecules [1–4]. In the following years, the discoveries of such resonances continued down to the lowest energies. For instance, the most recent published measurement of  $^{12}\text{C}+^{12}\text{C}$  fusion reported a strong resonance at  $E_{\text{c.m.}} = 2.14$  MeV [5].

Apart from its interest to nuclear reaction studies,  $^{12}\text{C}+^{12}\text{C}$  fusion reaction also plays a crucial role in a number of important astrophysical scenarios, such as explosions on the surfaces of neutron stars, white dwarf (type Ia) supernovae, and massive stellar evolution [6]. For astrophysics, the important energy range extends from 1 to 3 MeV in the center-of-mass frame, which is only partially covered by experiments. Therefore, an extrapolation is the only resource available to obtain the reaction rate for astrophysical applications. The currently adopted reaction rate is established based on the modified  $S$  factor  $S^*(E)$  [7], which is defined as,

$$S^*(E) = \sigma(E)Ee^{\frac{87.21}{\sqrt{E}} + 0.46E}. \quad (1)$$

An  $S^*$  factor of  $3 \times 10^{16}$  MeV b was obtained by fitting the data measured by Patterson [7], Spinka [8] and Becker [9].

This averaged value was extrapolated toward lower energies by assuming that the averaged  $S^*$  factor remains constant at sub-barrier energies [7,10]. At present, there is nothing known about the energies and strengths of resonances in the energy region below  $E_{\text{c.m.}} = 2$  MeV. Besides this uncertainty, the recent study of fusion hindrance has suggested a new extrapolation that is smaller than the adopted one [6,11]. Therefore, our understanding of the  $^{12}\text{C}+^{13}\text{C}$  fusion rate is highly uncertain.

In contrast to the striking resonances observed in the  $^{12}\text{C}+^{12}\text{C}$  fusion reaction, the other carbon systems, such as  $^{12}\text{C}+^{13}\text{C}$  and  $^{13}\text{C}+^{13}\text{C}$ , behave more regularly. Only minor resonance features have been observed in these two systems [12,13]. Although the  $^{12}\text{C}+^{12}\text{C}$  core-core interaction in the two isotope systems is identical to the one leading to the formation of the  $^{12}\text{C}+^{12}\text{C}$  molecular resonances, the presence of the valence nucleon(s) tends to smear resonances that would otherwise result from the core-core interactions [3]. Therefore, studies of  $^{12}\text{C}+^{13}\text{C}$  and  $^{13}\text{C}+^{13}\text{C}$  provide an opportunity to model the smooth behavior of the carbon fusion cross sections at deep sub-barrier energies.

### II. THE $^{12}\text{C}+^{13}\text{C}$ EXPERIMENT

As the first step, we studied  $^{12}\text{C}+^{13}\text{C}$  fusion in the center-of-mass energy range of 2.6 to 4.8 MeV using decay spectroscopy. A  $^{13}\text{C}$  beam with an intensity up to 1 particle  $\mu\text{A}$  was provided by the 10-MV FN Tandem accelerator at the University of Notre Dame. A gas stripper system was used to increase the intensity of the  $^{13}\text{C}$   $2^+$  charge state. The beam energies were determined from the magnetic field of the  $90^\circ$  analyzing magnet after the accelerator. The magnet was calibrated using

\* Current address: APC Muon Accelerator R&D, Fermilab, Batavia, IL.

† Deceased.

‡ x.tang@nd.edu

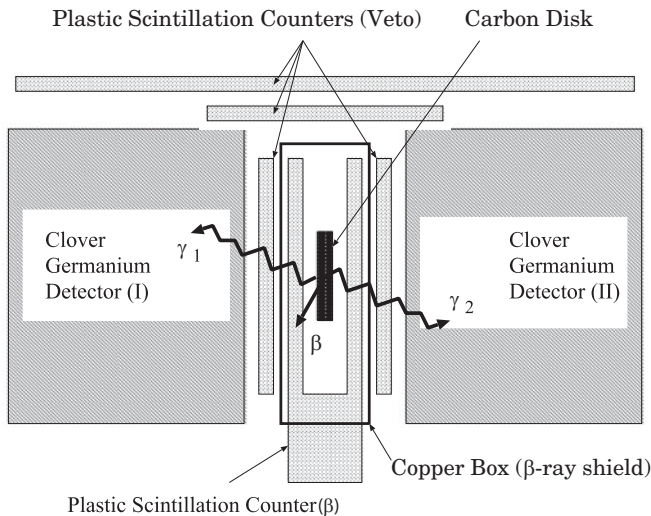


FIG. 1. Schematic view of the detector setup. The lead shielding is not shown in this figure.

$^{27}\text{Al}(p,n)$  and  $^{12}\text{C}(p,p)$  reactions. The  $^{13}\text{C}$  beam impinged on a 1-mm-thick natural carbon target. The cross sections for the  $^{12}\text{C}(^{13}\text{C},p)^{24}\text{Na}$  reaction were determined through measurement of the  $\beta$ -decay yield of  $^{24}\text{Na}$  ( $T_{1/2} = 14.9$  h) using the  $\beta$ - $\gamma$  coincidence method. The detector setup is shown in Fig. 1. The irradiated carbon target was sandwiched by two 1-mm-thick plastic scintillation counters to detect the  $\beta$  rays from  $^{24}\text{Na}$ . The cascading  $\gamma$  rays (1369- and 2754-keV) were detected by two Ge clover detectors. To stop the  $\beta$  particles from reaching the germanium detectors, the carbon target and the two plastic detectors were surrounded by a box made with 2-mm-thick copper sheets. The detection system was shielded with 7-cm-thick lead to reduce the cosmic ray background. Figure 2 shows typical  $\gamma$ -ray spectra obtained from the thick carbon target, which was irradiated at  $E(^{13}\text{C}) = 5.9$  MeV for 28 h. The  $\beta$ -ray gate allowed us to suppress the ambient background  $\gamma$  rays from natural radioactive isotopes such as  $^{40}\text{K}$  and  $^{208}\text{Tl}$ . The 1369- and 2754-keV peaks of  $^{24}\text{Na}$  were clearly observed in the  $\beta$ -gated  $\gamma$ -ray spectrum. Several plastic veto detectors had been used in this experiment to veto the cosmic ray background. However, the detection efficiency of the vetoed  $\beta$ - $\gamma$  coincidence became lower because these veto detectors were also sensitive to the  $\gamma$  rays. Therefore, we only chose  $\beta$ - $\gamma$  coincidence events without veto in our final analysis.

The thick-target yield ( $Y$ ) was obtained by normalizing the  $\beta$ -gated  $\gamma$ -ray yield to the total incident  $^{13}\text{C}$  flux. To extract the derivative  $dY/dE$  from the thick-target yield ( $Y$ ),  $dY/dE$  at a given energy was calculated by fitting this data point together with its two neighbors using a second-order polynomial in a  $\log Y$  versus  $E$  plot. This method was tested with a set of data simulated with GEANT4. The cross section for the  $^{12}\text{C}(^{13}\text{C},p)^{24}\text{Na}$  reaction was then calculated from the extracted  $dY/dE$  using the equation

$$\sigma(E) = \frac{1}{\varepsilon} \frac{M_T}{f N_A} \frac{dY}{dE} \frac{dE}{d(\rho X)}, \quad (2)$$

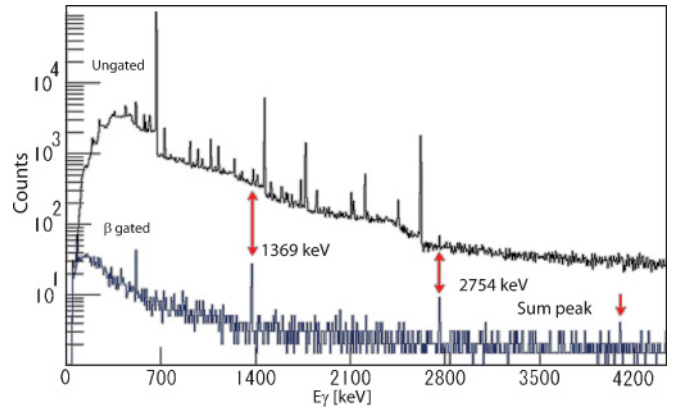


FIG. 2. (Color online) Comparison of two  $\gamma$ -ray spectra obtained with and without the  $\beta$ -ray gate. The  $^{24}\text{Na}$  sample was irradiated at  $E(^{13}\text{C}) = 5.9$  MeV for 28 h.

where  $\varepsilon$  is the detection efficiency of the  $\beta$ - $\gamma$  coincidence,  $M_T$  is the molecular weight of the target,  $f$  is the molecular fraction of the target nucleus of interest,  $N_A$  is Avogadro's number, and  $dE/d(\rho X)$  is the stopping power given by the SRIM code [14]. The detection efficiency  $\varepsilon$  was determined to be 2.0% by normalizing the observed cross section  $\varepsilon\sigma(E)$  at  $E_{c.m.} = 4.8$  MeV to the  $^{13}\text{C}(^{12}\text{C},p)^{24}\text{Na}$  cross section reported in Ref. [12]. The relative error is estimated to be 6%, which includes both uncertainties of the cross sections obtained from Ref. [12] and from this experiment.

The  $^{24}\text{Na}$  could also be produced via the  $^{13}\text{C}(^{13}\text{C},pn)^{24}\text{Na}$  reaction because the natural carbon target includes a 1.1% contamination of  $^{13}\text{C}$ . The cross sections for this reaction were measured down to  $E_{c.m.} = 3.5$  MeV [13] where the partial cross section for  $^{24}\text{Na}$  is  $0.86 \mu\text{b}$ , i.e., 7.6% of the cross section for the  $^{12}\text{C}(^{13}\text{C},p)^{24}\text{Na}$  reaction measured at the same  $^{13}\text{C}$  incident energy in this experiment. Thus the contribution from  $^{13}\text{C}+^{13}\text{C}$  to the total  $^{24}\text{Na}$  yield measured in this experiment is only  $8 \times 10^{-4}$ . Therefore, it is fairly reasonable to assume that the contribution from  $^{13}\text{C}+^{13}\text{C}$  remains negligible at lower energies.

In order to deduce the total cross section for compound nucleus formation for  $^{12}\text{C}+^{13}\text{C}$ , the theoretical branching ratio for the proton emission channel was used as correction factor [12]. The systematic uncertainty of the theoretical branching ratio is estimated to be 20% [12], which is the largest component in the error budget. Besides this systematic uncertainty, we also considered the statistical error, the uncertainty of beam normalization (5%), and the uncertainty of the  $\beta$ - $\gamma$  efficiency (6%). In this experiment, the lowest measured cross section has been pushed down from  $1 \mu\text{b}$  [12] to 20 nb. The results are shown in Fig. 3.

There is another measurement on  $^{12}\text{C}+^{13}\text{C}$  using the total- $\gamma$ -ray-yield method in the center-of-mass energy range of 3.1 to 6.7 MeV [15]. For energies  $4 < E_{c.m.} < 5$  MeV, the total fusion cross sections from this measurement are about 10% higher than the ones obtained from the Dayras measurement [12]. At lower energies, the total fusion cross section from this measurement gradually decreases to about 14% below the Dayras measurement [15]. Considering the 15% systematic error of Ref. [15] and the 30% systematic error quoted in the

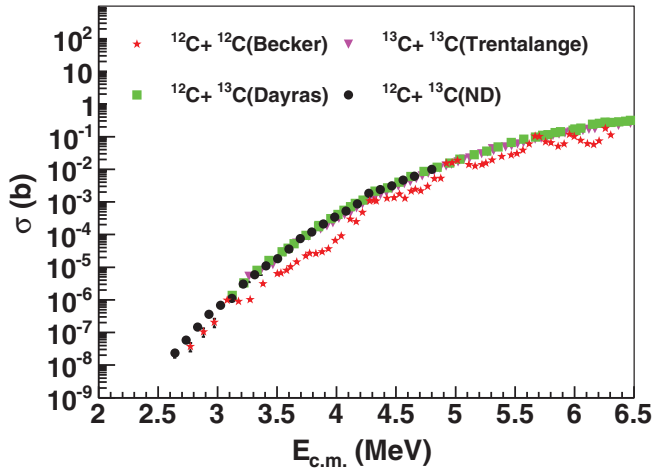


FIG. 3. (Color online) The fusion cross sections of three carbon isotope fusion reactions around or below the Coulomb barrier:  $^{12}\text{C} + ^{12}\text{C}$  (red stars) [9],  $^{12}\text{C} + ^{13}\text{C}$  from this work (black points) and Ref. [12] (green squares), and  $^{13}\text{C} + ^{13}\text{C}$  [13] (magenta triangles). The systematic uncertainties, 30% for the  $^{12}\text{C} + ^{12}\text{C}$  data, 15% for the  $^{13}\text{C} + ^{13}\text{C}$  data, and 30% for the  $^{12}\text{C} + ^{13}\text{C}$  data from Ref. [12] [ $^{12}\text{C} + ^{13}\text{C}$  (Dayras)], are not shown in the graph. The  $^{12}\text{C} + ^{13}\text{C}$  data reported in this paper [ $^{12}\text{C} + ^{13}\text{C}$ (ND)] are dominated by a 20% systematic uncertainty, which is included in this graph.

Dayras experiment [12], both works agree well with each other. Since our experiment requires the branching ratio information from the Dayras measurement [12], we can only normalize our data to the Dayras data at  $E_{c.m.} = 4.8$  MeV in order to avoid a double counting of the systematic errors.

### III. THE CORRELATION BETWEEN $^{12}\text{C} + ^{12}\text{C}$ , $^{12}\text{C} + ^{13}\text{C}$ , AND $^{13}\text{C} + ^{13}\text{C}$ FUSION CROSS SECTIONS

The shape of the fusion cross sections at sub-barrier energies is primarily dominated by the Coulomb barrier penetration effect. To remove this effect and reveal more details of the nuclear interaction, the cross sections of all three carbon fusion systems are converted into  $S^*$  factors using Eq. (1). The advantage of using this conversion over the traditional presentation with the astrophysical  $S$  factor [12] is that the cross-section ratios among the three systems are preserved in this representation. The results are shown in Fig. 4. There are several important features in these carbon-isotope fusion systems: (a) The observed cross sections for  $^{12}\text{C} + ^{12}\text{C}$  are the smallest of the three systems. They are bound from above by the cross sections of the other two carbon systems,  $^{12}\text{C} + ^{13}\text{C}$  and  $^{13}\text{C} + ^{13}\text{C}$ . (b) Considering a systematic uncertainty of 15–30% for the data from Refs. [9,12,13] (not shown in Fig. 4), the major resonant cross sections of  $^{12}\text{C} + ^{12}\text{C}$  ( $E_r = 3.1, 4.3, 4.9, 5.7, 6.0,$  and  $6.3$  MeV) match remarkably well with the fusion cross sections of the other two carbon isotope combinations within their quoted uncertainties. (c) Overall, the  $^{12}\text{C} + ^{13}\text{C}$  cross sections are the largest among the three carbon isotope fusion systems. Excluding the data point at 4.3 MeV in  $^{12}\text{C} + ^{13}\text{C}$ , the differences between  $^{12}\text{C} + ^{13}\text{C}$  and  $^{13}\text{C} + ^{13}\text{C}$  in the energy range of 3.5 to 5 MeV is less than 30%.

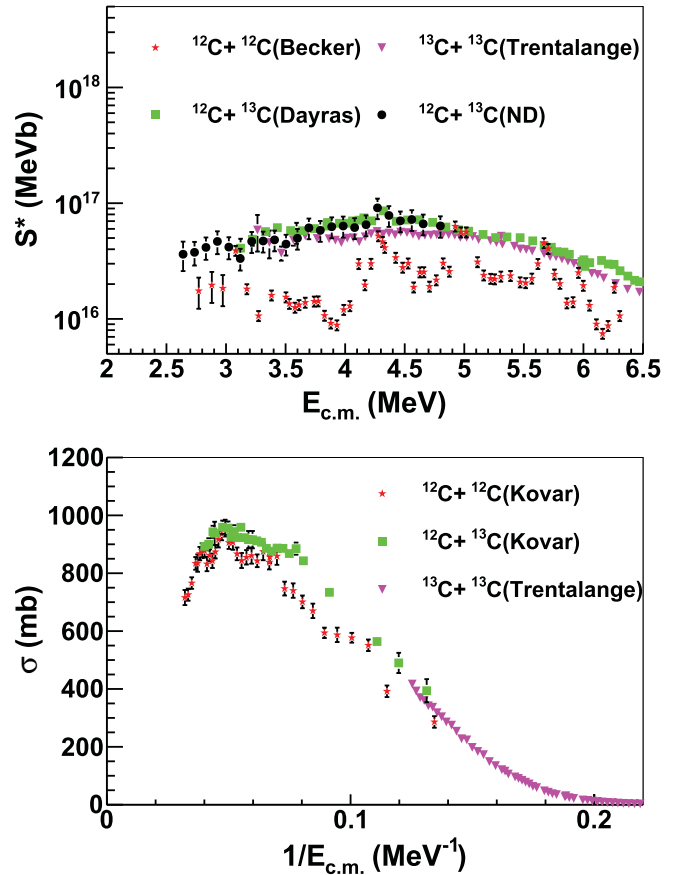


FIG. 4. (Color online) (top) The experimental  $S^*$  factors of three carbon-isotope fusion reactions around or below the Coulomb barrier:  $^{12}\text{C} + ^{12}\text{C}$  (red stars) [9],  $^{12}\text{C} + ^{13}\text{C}$  from this work (black points) and Ref. [12] (green squares), and  $^{13}\text{C} + ^{13}\text{C}$  [13] (magenta triangles). See the caption of Fig. 3 for a discussion on uncertainties. (bottom) The experimental cross sections of three carbon-isotope fusion reactions above the Coulomb barrier:  $^{12}\text{C} + ^{12}\text{C}$  (red points) [16],  $^{12}\text{C} + ^{13}\text{C}$  (green squares) [16] and  $^{13}\text{C} + ^{13}\text{C}$  [13] (magenta triangles).

The fusion cross sections of the three systems at energies above the Coulomb barrier show a similar behavior. Using the data from Refs. [13,16], the cross sections are plotted against the inverse of the center-of-mass energy as shown in Fig. 4. It is obvious that the cross sections for  $^{12}\text{C} + ^{13}\text{C}$  and  $^{13}\text{C} + ^{13}\text{C}$  still provide an upper limit for  $^{12}\text{C} + ^{12}\text{C}$  up to the highest measured energies. The trend of  $^{12}\text{C} + ^{13}\text{C}$  in a plot of  $\sigma$  versus  $1/E_{c.m.}$  agrees with the one of  $^{13}\text{C} + ^{13}\text{C}$  within their uncertainties.

We have fitted both  $^{12}\text{C} + ^{13}\text{C}$  and  $^{13}\text{C} + ^{13}\text{C}$  in the energy range of 4.9 to 8.0 MeV using the Wong formula [17]. The extracted fusion barrier parameters,  $R_b$ ,  $V_b$ , and  $\hbar\omega$  are summarized in Table I. The systematic uncertainties were included in the fit. It is evident that both systems have very similar fusion barriers. We also tried to fit the  $^{12}\text{C} + ^{12}\text{C}$  data from Ref. [9] at energies around the Coulomb barrier. However, because of the strong resonant structure, the fitting results strongly depend on the choice of fitting range. Therefore, no meaningful result could be achieved. Kovar *et al.* have fitted their  $^{12}\text{C} + ^{12}\text{C}$  and  $^{12}\text{C} + ^{13}\text{C}$  data using a simple classical fusion model in the energy range of  $1.1V_b$  to  $2V_b$  [16]. Because the fits were performed at energies above the Coulomb

TABLE I. List of the fusion barrier parameters  $R_b$ ,  $V_b$ , and  $\hbar\omega$  obtained in fits with the Wong formula [17]. The references from which the data were taken are given in the first column. For comparison, the fits from Ref. [16] are also included in this table. Since these fits were done at energies above the Coulomb barrier, no  $\hbar\omega$  parameter could be extracted.

Reaction	$R_b$ (fm)	$V_b$ (MeV)	$\hbar\omega$ (MeV)	Range (MeV)
$^{13}\text{C}+^{13}\text{C}$ [13]	$6.5 \pm 0.5$	$5.6 \pm 0.1$	$2.1 \pm 0.3$	4.9 – 8.0
$^{12}\text{C}+^{13}\text{C}$ [12]	$7.4 \pm 0.5$	$5.7 \pm 0.1$	$2.1 \pm 0.3$	4.9 – 8.0
$^{12}\text{C}+^{13}\text{C}$ [16]	$7.0 \pm 0.2$	$5.7 \pm 0.3$		$1.1V_b - 2V_b$
$^{12}\text{C}+^{12}\text{C}$ [16]	$6.5 \pm 0.4$	$5.8 \pm 0.3$		$1.1V_b - 2V_b$

barrier, the  $\hbar\omega$  parameter could not be determined. Their determined  $R_b$  and  $V_b$  agree with our results within their quoted uncertainties.

At energies above the Coulomb barrier, the resonant-like structure in the  $^{12}\text{C}+^{12}\text{C}$  cross sections has been well studied and is reviewed in Ref. [3]. In this paper, we shall concentrate our discussion on the correlation between the peak cross sections in  $^{12}\text{C}+^{12}\text{C}$  and the cross sections of the other two carbon-isotope systems at energies below the Coulomb barrier.

#### IV. COUPLED-CHANNELS CALCULATIONS USING THE INGOING WAVE BOUNDARY CONDITION (IWBC)

In this section we discuss coupled-channels calculations for the three systems using two different potentials. Before we present our results, it is important to briefly review the ingoing wave boundary condition (IWBC) used in our calculations [18]. In this approach, the fusion system is treated as a “black body” once the two nuclei in the fusion process overlap significantly. At the minimum position of the Coulomb plus nuclear potential pocket inside the barrier, the wave function for each partial wave has only ingoing components. This approximation is valid for most heavy-ion fusion reactions in which there is a strong absorption inside the Coulomb barrier. There is no provision within the IWBC for describing the resonant structure in the  $^{12}\text{C}+^{12}\text{C}$  reaction. This approximation has been used to describe the average trend in the  $^{12}\text{C}+^{12}\text{C}$ ,  $^{12}\text{C}+^{16}\text{O}$ , and  $^{16}\text{O}+^{16}\text{O}$  fusion reactions. Reasonable fits have been achieved for these three systems by adjusting the interaction potential [18]. However, with the presence of resonances, the choice of the nuclear potential is somewhat ambiguous.

The first potential used in the calculations is the Akyüz-Winther potential [19], which is an empirical global potential frequently used for fusion reactions at energies around the Coulomb barrier. The coupled-channels calculation (CC-AW) was done using the CCFULL code [20]. In the calculation, both the  $^{12}\text{C}(2^+, 4.44 \text{ MeV})$  and the  $^{13}\text{C}(3/2^-, 3.684 \text{ MeV})$  states are included. The results are shown by the dot-dashed lines in Fig. 5. A scaling factor of 0.8 has been used in all three systems to normalize the predicted cross sections to the experimental data. This deviation is comparable with the quoted experimental errors ( $\sim 30\%$ ). At  $E_{\text{c.m.}} > 5 \text{ MeV}$ , the CC-AW calculation provides a good description of the

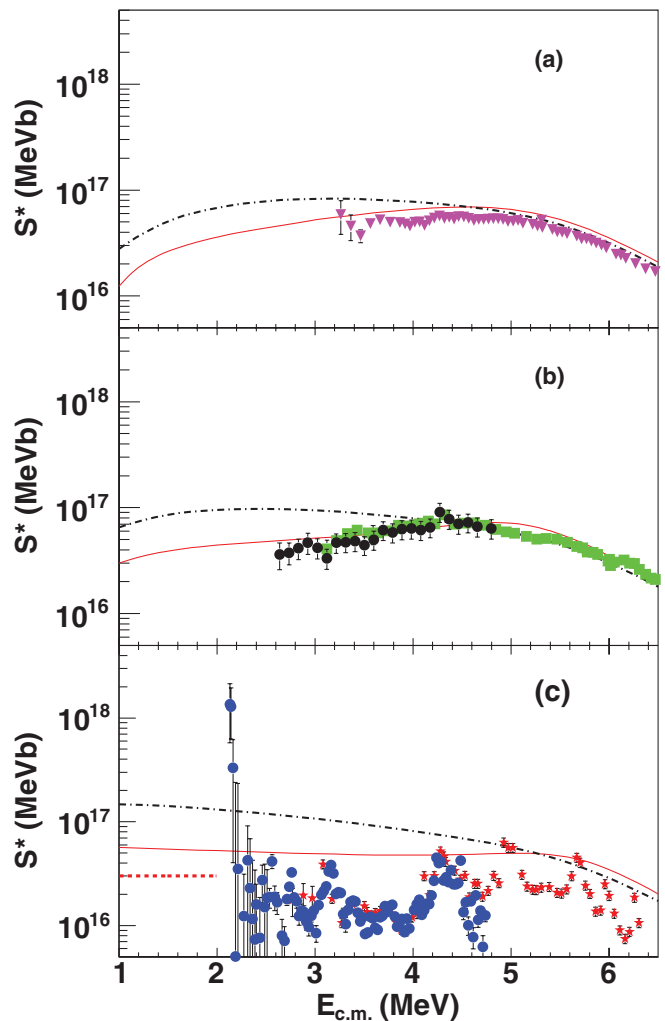


FIG. 5. (Color online) Comparisons between the experimental cross sections and the two coupled-channels calculations, CC-AW(dot-dashed line) and CC-M3Y + Rep (red solid line). (a), (b), and (c) correspond to  $^{13}\text{C}+^{13}\text{C}$ ,  $^{12}\text{C}+^{13}\text{C}$ , and  $^{12}\text{C}+^{12}\text{C}$ , respectively. The symbols for the various experimental data are identical to ones in Fig. 4. In (c), the data from Ref. [5] are shown by blue circles. The CC-AW calculations for all three systems are scaled by a factor of 0.8 to provide a better agreement with the experimental data. The adopted  $S^*$  factor ( $3 \times 10^{16} \text{ MeV b}$ ) at low energies is shown by the red dashed line.

fusion cross sections for  $^{12}\text{C}+^{13}\text{C}$  and  $^{13}\text{C}+^{13}\text{C}$  as well as the peak cross sections in  $^{12}\text{C}+^{12}\text{C}$ . At energies below 4–5 MeV, however, this calculation significantly over-predicts the cross sections for all three systems. If transfer channels would have been included, the deviations between the predicted and observed cross sections would further increase. This phenomenon is known as the fusion hindrance effect, which seems to be a universal phenomenon at energies significantly below the Coulomb barrier [11,21].

An improved coupled-channels calculation (CC-M3Y + Rep) has recently been performed using the M3Y potential with a repulsive core [21]. The  $^{12}\text{C}+^{13}\text{C}$  and  $^{13}\text{C}+^{13}\text{C}$  data were used to constrain the effective nuclear potential, which was then used for the calculation of the

fusion cross sections of the  $^{12}\text{C}+^{12}\text{C}$  system with the CC formula. The coupling effects from all the possible excited states with large deformation parameters as well as the transfer channels are included. Details of the calculation are presented in a separate paper [22]. Here we focus on the results shown by the solid red lines in Fig. 5. It is clear that the CC-M3Y + Rep calculation provides an excellent description for the  $^{12}\text{C}+^{13}\text{C}$  and  $^{13}\text{C}+^{13}\text{C}$  systems. The overall deviations are less than 30%, which is comparable with the experimental uncertainties. Using this constrained  $^{12}\text{C}+^{12}\text{C}$  nuclear potential, the coupled-channels calculation is able to predict all the major  $^{12}\text{C}+^{12}\text{C}$  peak cross sections reported in Ref. [9] with deviations of less than 30%.

The recently published low-energy data points from Ref. [5] are also included in Fig. 5(c). It is obvious that our CC-M3Y + Rep calculation [see red solid line in Fig. 5(c)] provides an excellent upper limit for almost all the data except for the two data points around 2.14 MeV. These two points are also well above the CC-AW calculation, which seems to always over-predict fusion cross sections at deep sub-barrier energies [11].

The measurement of Ref. [5] was a very challenging experiment. From 2.1 to 2.75 MeV, the cross sections are of the order of a few nb or less. The efficiency of the  $\gamma$  detector was low (3.9% for the 440 keV line and 1.9% for the 1.634 MeV line). Limited by these factors, the statistics of the nine data points within this energy range were poor. Most of them have uncertainties reaching 100%. The claim for the existence of the strong resonance at 2.14 MeV relies on two data points in the  $\alpha$  channel with  $S^* = (1.4 \pm 0.8) \times 10^{18}$  MeV b at 2.131 MeV and  $(1.0 \pm 0.6) \times 10^{18}$  MeV b at 2.144 MeV, and one data point in the proton channel,  $(0.3 \pm 0.2) \times 10^{18}$  MeV b at 2.163 MeV [5]. According to the so-called Bad-Honnef statement, one important criterion for a molecular resonance is the appearance of an increased angle-integrated cross section in at least two exit channels [23]. Therefore, this data point in the proton channel is important since it indicates that this resonance is a candidate for a new molecular resonance in the  $^{12}\text{C}+^{12}\text{C}$  entrance channel.

The  $^{12}\text{C}(^{12}\text{C},p)$  reaction has been remeasured at Naples by the same group in the energy range of  $2.1 < E_{\text{c.m.}} < 4$  MeV [24]. In this experiment, it was found that the deuterium contamination in the regular graphite target, which was claimed to be totally eliminated by heating the target in the previous measurement [5], produces significant background that complicates measurements below  $E_{\text{c.m.}} \approx 2.6$  MeV. It was also found that a highly ordered pyrolytic graphite (HOPG) target has a much lower hydrogen level, with which they were able to extend their measurements down to  $E_{\text{c.m.}} = 2.1$  MeV [25]. Their preliminary result shows a much smaller  $S^*$  factor for the proton channel,  $(0.6 \pm 1.4) \times 10^{16}$  MeV b at 2.15 MeV. This new  $S^*$  factor for the proton channel is about a factor of 50 less than the previously reported value [24]. The deuterium contamination is not necessarily the explanation for the large discrepancy. However, the disappearance of the resonance in the proton channel unambiguously shows that the beam-induced background, which was ignored in Ref. [5], is significant enough to question the resonance reported in Ref. [5].

In order to get the total  $S^*$  factors from the measured proton channel data, the proton decay branching ratio measured at higher energies ( $E_{\text{c.m.}} > 2.8$  MeV) [9] was extrapolated down to lower energies. The new total  $S^*$  factor at 2.15 MeV was determined to be  $(1.4 \pm 3.3) \times 10^{16}$  MeV b [24]. This new result agrees well with our predicted upper limit which is about  $S^* = 5.8 \times 10^{16}$  MeV b for  $E_{\text{c.m.}} < 2.2$  MeV [see Fig. 5(c)].

## V. DISCUSSIONS

It is interesting to note that the CC-M3Y + Rep prediction using a constrained  $^{12}\text{C}+^{12}\text{C}$  nuclear potential does not describe the average trend of the cross sections, but rather matches the observed  $^{12}\text{C}+^{12}\text{C}$  peak cross sections. This is different from the treatment used in Ref. [26], where the data are described by a series of Breit-Wigner resonances superimposed on a smooth nonresonant background.

Here we provide a qualitative explanation for our results, which is based on the intrinsic excited nuclear molecule model (Nogami-Imanishi model) [3,4,27–29]. In this model, the  $^{12}\text{C}(\text{g.s.})+^{12}\text{C}(2^+, 4.44 \text{ MeV})$  compound states are formed when 4.44 MeV of kinetic energy is temporarily converted into internal excitation energy, thereby lowering the relative motion into a quasibound molecular orbit in the internuclear potential. These quasimolecular states can then either decay back into the incident channel or into the compound nucleus  $^{24}\text{Mg}$ . By including the coupling effect between the elastic channel and the single excitation channel that forms the quasimolecular states, Imanishi was able to reproduce the characteristics of the three resonances found in Ref. [1]. This model was subsequently generalized to provide a qualitative description for the molecular resonances at energies both below and above the Coulomb barrier [3,4]. Kondon, Matsuse, and Abe in their band-crossing model (BCM) took into account the excitation of both  $^{12}\text{C}$  nuclei and extended the calculation to the energy range of  $4 < E_{\text{c.m.}} < 7$  MeV [29]. Their model could reproduce the characteristic features of the total reaction cross section, i.e., resonance widths, peak heights, level densities of the resonances, and the energy dependence of the averaged total reaction cross sections. In this calculation, only three rotational eigenstates with  $L = 0, 2,$  and  $4$  were included in elastic, single, and mutual excited channels. However, with these coupling effects, they obtained a rich resonant structure with 14 resonances in the range of  $4 < E_{\text{c.m.}} < 7$  MeV. The level spacing is about 200 keV, which is wider than the resonance widths ( $\sim 100$  keV).

Because of the low level density in the  $^{12}\text{C}+^{12}\text{C}$  system, the coupling effects leading to the formation of quasimolecular states can only take place at certain energies. At these resonant energies, our CC-M3Y + Rep calculations suggest that the complicated  $^{12}\text{C}+^{12}\text{C}$  system can be interpreted as a simple strong absorption system that absorbs all the ingoing fluxes from both the incident channel and the coupled inelastic channels.

For  $^{12}\text{C}+^{13}\text{C}$  and  $^{13}\text{C}+^{13}\text{C}$ , the coupling effects to the excited  $^{12}\text{C}$  core should also exist. For example, the  $^{13}\text{C}(3/2^-, 3.684 \text{ MeV})$  state included in our coupled-channels calculation can be interpreted as an oblate  $^{12}\text{C}$  core with its 4.44 MeV

( $2^+$ ) state coupled to a  $p_{1/2}$  valence neutron [22]. However, the resonance structures that should also exist in these two systems disappear due to the coupling of the valence neutron in  $^{13}\text{C}$ . This result may not be so surprising. On the experimental side, the effect of valence neutron(s) has been well studied in various reaction processes. For elastic scattering, Beck *et al.* observed that the resonant structure in the excitation function of  $^{28}\text{Si}+^{28}\text{Si}$  is completely washed out by the valence neutrons in  $^{28}\text{Si}+^{30}\text{Si}$  and  $^{30}\text{Si}+^{30}\text{Si}$  [30]. In inelastic scattering, the structure of the excitation function of  $^{12}\text{C}+^{18}\text{O}$  is less pronounced than the one observed in the  $^{12}\text{C}+^{16}\text{O}$  data, while the  $^{13}\text{C}+^{17}\text{O}$  system shows very little structure [3]. It has also recently been observed that structures in the barrier distribution for the quasielastic scattering of  $^{20}\text{Ne}+^{90,92}\text{Zr}$  change dramatically due to a large number of noncollective excitations [31]. On the theory side, it is known that the coupling of the valence neutron(s) to the  $^{12}\text{C}+^{12}\text{C}$  cores in  $^{12}\text{C}+^{13}\text{C}$  and  $^{13}\text{C}+^{13}\text{C}$  dramatically increases the resonance widths and the level densities of the compound nuclei. Haas and Abe investigated the number of open channels (NOC), the ratio of resonance width to the level spacing between resonances, for a number of systems [32,33]. Among these systems, they found that the NOC in  $^{12}\text{C}+^{12}\text{C}$  is the lowest while the NOCs of  $^{12}\text{C}+^{13}\text{C}$  and  $^{13}\text{C}+^{13}\text{C}$  are almost two orders of magnitude higher than that of  $^{12}\text{C}+^{12}\text{C}$ . With such high level density in the  $^{12}\text{C}+^{13}\text{C}$  and  $^{13}\text{C}+^{13}\text{C}$  systems, the coupling effect may take place at any energy. Therefore, these two systems are expected to behave like strong absorption systems and exhibit a similar behavior in the fusion cross sections over a wide energy range. However, for the  $^{12}\text{C}+^{12}\text{C}$  system, the fusion cross sections are suppressed because of its low level density and are limited from above by the cross sections of  $^{12}\text{C}+^{13}\text{C}$  and  $^{13}\text{C}+^{13}\text{C}$ .

In order to provide a more accurate prediction at deep sub-barrier energies, it is urgent to improve experimental techniques so that the measurements of the fusion reactions among carbon isotopes can be pushed toward lower energies.

Right now, the Notre Dame group is building a new 5 MV accelerator with an Electron Cyclotron Resonance source to provide high-current carbon beams. With improvements of the detection techniques [34], better experimental data can be expected in the near future.

## VI. SUMMARY

To summarize, an empirical relationship among the fusion cross sections for the three carbon isotope systems,  $^{12}\text{C}+^{12}\text{C}$ ,  $^{12}\text{C}+^{13}\text{C}$ , and  $^{13}\text{C}+^{13}\text{C}$ , has been found. After calibrating the M3Y + Rep effective potential, the coupled-channels calculation with the IWBC (CC-M3Y + Rep) is able to provide a quantitative description for the peak cross sections in  $^{12}\text{C}+^{12}\text{C}$ . This finding can be qualitatively understood with the Nogami-Imanishi model and the level density differences in the compound nuclei. We set an upper limit for the  $^{12}\text{C}+^{12}\text{C}$  fusion cross section in the range of  $E_{\text{c.m.}} > 2.1$  MeV, which agrees with all the experimental data except for the strong resonance observed at 2.14 MeV. This system has recently been remeasured, yielding a smaller cross section that agrees with our predictions [24]. The extrapolated upper limit puts a useful constraint on the carbon fusion cross sections at lower energies, which are important for astrophysical applications.

## ACKNOWLEDGMENTS

This work was supported by the NSF under Grants No. PHY-0758100 and No. PHY-0822648, the DOE office of Science through Grant No. DE-AC02-06CH11357, the National Natural Science Foundation of China under Grant No. 11021504, and the University of Notre Dame. Stimulating discussions with M. Wiescher, J. Kolata, S. Trentalange, H. Spinka, M. Beard, K. Hagino, J. P. Schiffer, B. Imanishi, W. von Oertzen, M. Freer, K. Langanke, Y. Abe, G. Imbriani, and J. Zickefoose are gratefully acknowledged.

- 
- [1] E. Almqvist, J. A. Kuehner, and D. A. Bromley, *Phys. Rev. Lett.* **4**, 515 (1960).
  - [2] D. A. Bromley, *Sci. Am.* **230**, 58 (1978).
  - [3] K. A. Erb and D. A. Bromley, *Treatise on Heavy-Ion Science*, edited by D. A. Bromley (Plenum Press, New York, 1985), Vol. 3, Chap. 3, pp. 201–310.
  - [4] W. Greiner, J. Y. Park, and W. Sheid, *Nuclear Molecules* (World Scientific, Singapore, 1995).
  - [5] T. Spillane *et al.*, *Phys. Rev. Lett.* **98**, 122501 (2007).
  - [6] L. R. Gasques *et al.*, *Phys. Rev. C* **76**, 035802 (2007).
  - [7] J. R. Patterson, H. Winkler, and C. S. Zaidins, *Astrophys. J.* **157**, 367 (1969).
  - [8] H. Spinka and H. Winkler, *Nucl. Phys. A* **233**, 456 (1974).
  - [9] H. W. Becker, K. U. Kettner, C. Rolfs, and H. P. Trautvetter, *Z. Phys. A* **303**, 305 (1981).
  - [10] G. R. Caughlan and W. A. Fowler, *At. Data Nucl. Data Tables* **40**, 283 (1988).
  - [11] C. L. Jiang, K. E. Rehm, B. B. Back, and R. V. F. Janssens, *Phys. Rev. C* **75**, 015803 (2007).
  - [12] R. A. Dayras, R. G. Stokstad, Z. E. Switkowski, and R. M. Wieland, *Nucl. Phys. A* **265**, 153 (1976).
  - [13] S. Trentalange, S. C. Wu, J. L. Osborne, and C. A. Barnes, *Nucl. Phys. A* **483**, 406 (1988).
  - [14] L. Barron-Palos *et al.*, *Nucl. Phys. A* **779**, 318 (2006).
  - [15] B. Dasmahapatra, B. Cujec, and F. Lahlou, *Nucl. Phys. A* **384**, 257 (1982).
  - [16] D. G. Kovar *et al.*, *Phys. Rev. C* **20**, 1305 (1979).
  - [17] C. Y. Wong, *Phys. Rev. Lett.* **31**, 766 (1973).
  - [18] P. Christensen and Z. Switkowski, *Nucl. Phys. A* **280**, 205 (1977).
  - [19] Ö. Akyüz and A. Winther, in *Nuclear Structure and Heavy-Ion Collisions*, Proceedings of the International School of Physics “Enrico Fermi,” Course LXXVII, edited by R. A. Broglia, R. A. Ricci, and C. H. Dasso (North-Holland, Amsterdam, 1981).
  - [20] K. Hagino, N. Rowley, and A. Kruppa, *Comput. Phys. Commun.* **123**, 143 (1999), and references therein.
  - [21] S. Misiu and H. Esbensen, *Phys. Rev. C* **75**, 034606 (2007).

- [22] H. Esbensen, X. Tang, and C. L. Jiang, [Phys. Rev. C \*\*84\*\*, 064613 \(2011\)](#).
- [23] *Resonances in Heavy Ion Reactions (Bad Honnef, Germany, 1981)*, edited by K. A. Eberhard, Lecture Notes in Physics, Vol. 156 (Springer, Berlin, Germany, 1981).
- [24] J. Zickefoose, Ph.D. Thesis, University of Connecticut (unpublished).
- [25] J. Zickefoose *et al.*, in *Proceedings of the 11th Symposium on Nuclei in the Cosmos*, PoS(NIC XI)019.
- [26] E. F. Aguilera *et al.*, [Phys. Rev. C \*\*73\*\*, 064601 \(2006\)](#).
- [27] B. Imanishi, [Phys. Lett. B \*\*27\*\*, 267 \(1968\)](#).
- [28] B. Imanishi, [Nucl. Phys. A \*\*125\*\*, 33 \(1969\)](#).
- [29] Y. Kondo, T. Matsuse, and Y. Abe, [Prog. Theor. Phys. \*\*59\*\*, 465 \(1978\)](#).
- [30] C. Beck, Y. Abe, N. Aissaoui, B. Djerroud, and F. Haas, [Phys. Rev. C \*\*49\*\*, 2618 \(1994\)](#).
- [31] E. Piasecki *et al.*, [Phys. Rev. C \*\*80\*\*, 054613 \(2009\)](#).
- [32] F. Haas and Y. Abe, [Phys. Rev. Lett. \*\*46\*\*, 1667 \(1981\)](#).
- [33] B. Heusch *et al.*, [Phys. Rev. C \*\*23\*\*, 1527 \(1981\)](#).
- [34] C. L. Jiang, [EPJ Web Conf. \*\*17\*\*, 01002 \(2011\)](#).